Design of S-band re-entrant cavity BPM

LUO Qing SUN Baogen* HE Duohui

National Synchrotron Radiation Laboratory, School of Nuclear Science and Technology, University of Science and Technology of China, Hefei 230029, China

Abstract An S-band cavity BPM is designed for a new injector for HLS (Hefei Light Source). It consists of two cavities that work on 2448 MHz: a re-entrant position cavity tuned to TM110 mode and a reference cavity tuned to TM010 mode. Cut-through waveguides are used as pickups to suppress the monopole signal. Simulations with different assumption of dimension change are performed to evaluate errors caused by mechanical error and give general tolerance. Design of electronics is given. Theoretical resolution of this design is 31 nm.

Key words Cavity BPM, Re-entrant, Cut-through waveguide, MAFIA, Omega3p, AD8302

1 Introduction

The high brightness injector of HLS (Hefei Light Source) requests high precision control of the beam position and positional resolution of the beam position monitor (BPM) for the photocathode RF gun of the injector should be better than 10 μm. For a substantial improvement in positional resolution of the BPM system, NSRL decided to use cavity BPM, which promises much higher position resolution than other types of BPM, such as the stripline BPM used at HLS before[1,2].The cavity BPM system designed by KEK and tested at SLC has achieved a resolution of 25 nm, while it may reach 1 nm, theoretically [3].

A cavity BPM is a cylindrical cavity as pick-up station in the beam-pipe. When an off-centered beam passes through the cavity, it excites electromagnetic field of a series of eigen modes (such as TM110 mode, see Fig. 1). In general, the signal that the electronics detected from TM110 mode has a linear dependence on absolute value of bunch displacement [2-7]. A reference cavity tuned to TM010 mode is needed for reading the sign of bunch displacement.

In our design, a re-entrant position cavity, instead of an ordinary pill-box cavity, is used to reduce the system size and the Q factor as well. Theoretically, the position resolution is 7 nm. With a noise factor of 10 from the electronics, the final resolution is 31 nm.

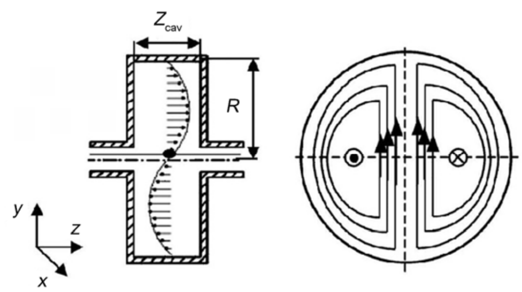

Fig. 1 Sketch of pick-up station and dipole mode.

2 Cavity BPM theory

When a beam bunch passes through a cavity, the energy loss, E_{loss}, satisfies:

$$E_{\text{loss}} = q^2 k_{\text{loss}} = q^2 \frac{\left(V_n(\vec{r},v)\right)^2}{4W_n}$$
$$V_n(\vec{r},v) = \int_0^l \mathrm{d}z\, E_n(\vec{r},v)\, e^{j\omega_n z/v} \qquad (1)$$

where k_{loss} is loss factor, v is velocity of bunch, q is bunch charge, l is cavity length, and $\vec{r}$ is displacement vector. To every eigen mode, E_n is electric filed intensity, ω_n is pulsatance, W_n is the energy stored in the eigenmode, and n shows the order of the eigenmode.

Supported by the Natural Science Foundation of China (10875117) and the National “985 Project” (173123200402002)

* Corresponding author. *E-mail address:* bgsun@ustc.edu.cn

Received date: 2008-12-15

E_n and W_n depend only on the cavity shape. For TM110 mode,

$$\vec{E}_n = C_{110} J_1(a_{11} r/R) \cos\varphi \; e^{-j\omega z} \tag{2}$$

where a_{11} is the first root of first order Bessel function, r is bunch displacement and R is cavity radius. For a relativistic beam bunch, ($a_{11}r/R$) is very small[4], then

$$V_n(\vec{r}, v) \propto J_1(a_{11} r/R) \propto r \tag{3}$$

In the cavity TM110 mode, the bunch energy loss is proportional to the square of bunch displacement. For a given BPM system, the power is proportional to the energy loss and the voltage detected by the BPM is proportional to the square root of the power. In general, it is agreed that the signal voltage detected in the TM110 mode is proportional to the bunch charge and displacement[4,5]. The signal voltage we get can be expressed as:

$$\begin{aligned} V_{\text{cavity}}(\omega_{110}) &= V_{110}^{\text{out}}(r) + V_{\text{monopole}} + V_{110}(\theta) + V_{\text{noise}} \\ &= jA_1 qr + jA_2 q + jA_3 q\theta + V_{\text{noise}} \end{aligned} \tag{4}$$

where ω_{110} is the resonant frequency of TM110 mode. The first term is useful output that we really need. The second term is common-mode leakage, the third term shows the effect of beam angle θ (both have 90° phase separation from beam intensity), and the last term usually is thermal noise.

A reference cavity tuned to TM010 mode is used to read the bunch displacement. It also helps to normalize the signal by the charge q.

The position resolution is the minimum displacement for the electronics to get a signal voltage higher than thermal noise. If the electronics is ideal (noise factor NF =1 and all the energy loss in TM110 mode is coupled out to the electronics[8]), there will be

$$\begin{aligned} V_{110}^{\text{out}} &= qr\left(Z_0 \frac{k_{\text{loss, normalized}}}{2} \frac{\omega_{110}}{Q_L} \frac{\beta}{1+\beta}\right)^{1/2} \\ V_{\text{noise}} &= (4 Z_0 kT \Delta F)^{1/2} \end{aligned} \tag{5}$$

where, $k_{\text{loss, normalized}}$ is loss factor of TM110 mode, normalized by bunch displacement, Z_0 is characteristic impedance of electronics, Q_L is loaded Q, β is the coupling factor (the ratio between no load Q and external Q), and ΔF is bandwidth of the electronics.

$\Delta F = f_0/Q_L$, where f_0 is center frequency of electronics. If f_0 equals to f_{110}, the ideal resolution is given by:

$$\Delta x_{\text{ideal}} = q^{-1}\left(\frac{\pi}{4kT} \frac{\beta}{1+\beta} k_{\text{loss, normalized}}\right)^{-1/2} \tag{6}$$

2.1 Coupling method selection

As the bunch displacement is very small, the TM010 signal is many orders of magnitude larger than the TM110 signal. To avoid the adverse impact on resolution from the TM010 mode, leakage waveguides are used as coupling method. In the area of coupling slots in Fig. 2, normal direction of waveguide surface is the same as direction of TM010 mode magnetic field, hence no surface conduction current on waveguide surface for TM010 mode. So monopole mode cannot be coupled to the waveguides. In addition, a waveguide cut off frequency between TM010 and TM110 mode resonance frequency of our cavity will help to suppress the TM010 mode signal.

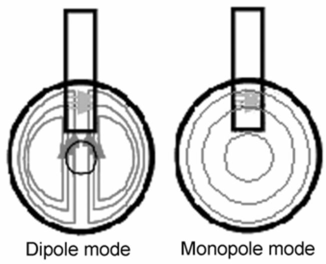

Fig. 2 Sketch of dipole mode and monopole mode.

Feed-throughs are used to pick up signals from waveguides. If feed-throughs does not match the waveguides, they would lead to resonance mode of waveguides that have a frequency close to dipole mode. There are two different ways to distinguish TM110 mode from other modes. One is to use feed-throughs matching the waveguides to eliminate waveguide modes and obtain a clear spectrum, which demands higher accuracy. The other is to move the frequency of waveguide modes far away from the frequency of TM110 mode, which is easier to achieve. Waveguides cutting through the beam pipe are used to reduce the frequency of waveguide mode in our design (Fig. 3).

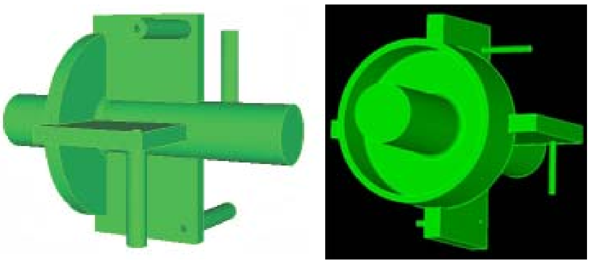

Fig. 3 Cut-through waveguide and re-entrant cavity.

2.2 Re-entrant cavity

A re-entrant cavity is used as position cavity in this design. It has much smaller size and much lower Q factor than a pill-box cavity (Table 1). Obviously, a beam lose less energy in the re-entrant cavity, size of the system can be controlled and proper waveguide be chosen easily.

Table 1 Comparison between re-entrant cavity and ordinary pill-box cavity

Cavities	Radius / mm	Q_{010}	Q_{110}	f_{010} / MHz	f_{110} / MHz
Re-entrant	47.9	2575.8	3110.4	1714.4	2302.3
Pill-box	75.6	5248.2	6515.4	1588.2	2302.3

3 Structure design

3.1 External *Q* study

External Q is an inherent parameter of the whole pick-up station. For pick-up station with given structure (fixed Q_0 and total energy loss) and electronics with given bandwidth, signal voltage detected by electronics will be very low whether Q_e is too large or too small. So there is at least a certain external Q value that enables the electronics to get the maximum signal voltage.

The signal voltage decays in the electronics as

$$V = V_0 \mathrm{e}^{-\frac{\omega_{110}}{2Q_L}t} \mathrm{e}^{j\omega_{110}t} \tag{7}$$

where V_0 is the starting voltage. The energy spectral density will be

$$P(\omega) = \frac{V_0^2}{2\pi} \frac{1}{[\omega_{110}/(2Q_L)]^2 + (\omega-\omega_{110})^2} \tag{8}$$

Then,

$$\int_{-\infty}^{\infty} P(\omega)\mathrm{d}\omega = V_0^2 \frac{Q_L}{\omega_{110}} \tag{9}$$

We also have

$$\begin{aligned}\int_{-\infty}^{\infty} P(\omega)\mathrm{d}\omega &= E_{\mathrm{output}} \\ &= k_{\mathrm{loss,\,normalized}}\, q^2 r^2 \frac{\beta}{1+\beta} \\ &= E_{\mathrm{loss}} \frac{\beta}{1+\beta}\end{aligned} \tag{10}$$

where E_{output} is energy coupled out and E_{loss} is total energy loss defined before. E_{loss} is a constant when displacement and charge are fixed. When center frequency of the electronics f_e is the same as the resonant frequency f_{110}, the energy that the electronics gets will be:

$$\begin{aligned}E_e &= \int_{\omega_{110}-\pi\Delta F}^{\omega_{110}+\pi\Delta F} P(\omega)\mathrm{d}\omega \\ &= V_0^2 \frac{Q_L}{\pi\,\omega_{110}}\, 2\,\mathrm{arctg}\left(\frac{\pi\Delta F}{\omega_{110}/(2Q_L)}\right) \\ &= E_{\mathrm{loss}} \frac{\beta}{1+\beta} \frac{2}{\pi} \mathrm{arctg}\left(\frac{\pi\Delta F}{\omega_{110}/(2Q_L)}\right)\end{aligned} \tag{11}$$

The ratio between energy in electronics and total energy loss is

$$Ratio = \frac{2}{\pi}\,\mathrm{arctg}\left(\frac{\Delta F\, Q_L}{f_{110}}\right) \frac{Q_0 - Q_L}{Q_0} \tag{12}$$

Fig. 4 shows dependence of the ratio to loaded Q at the bandwidth = 10 MHz, f_{110} = 2448 MHz, and Q_0 is about 3920. Set the differential coefficient of energy function equal to zero, solve this equation, a root of 747.8 can be found. It was decided to use an external Q of 300 and loaded Q would be around 280. Q_0 is much larger than Q_e, so Q_L is mainly decided by Q_e.

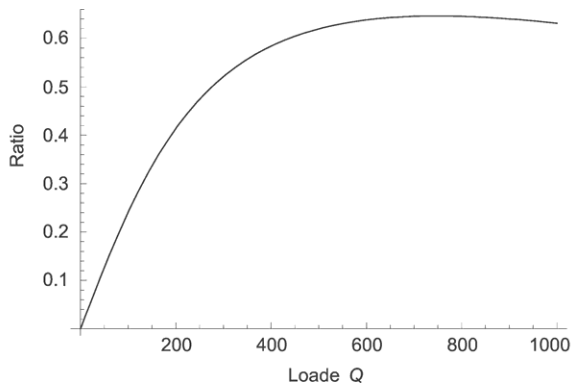

Fig. 4 Ratio between effective energy loss and total energy loss *vs*. loaded *Q*.

If f_{110} is different from center frequency of electronics f_e, the ratio function will be:

$$Ratio=\frac{1}{\pi}\frac{Q_0-Q_L}{Q_0}\left(\operatorname{arctg}\left(\frac{2\left(f_e+\frac{\Delta F}{2}-f_{110}\right)Q_L}{f_{110}}\right)-\operatorname{arctg}\left(\frac{2\left(f_e-\frac{\Delta F}{2}-f_{110}\right)Q_L}{f_{110}}\right)\right) \tag{13}$$

Fig. 5 shows that the energy coupled to electronics changes with the resonance frequency. It can be seen that when f_{110} displacement is in a range of 1MHz, its effect is negligible.

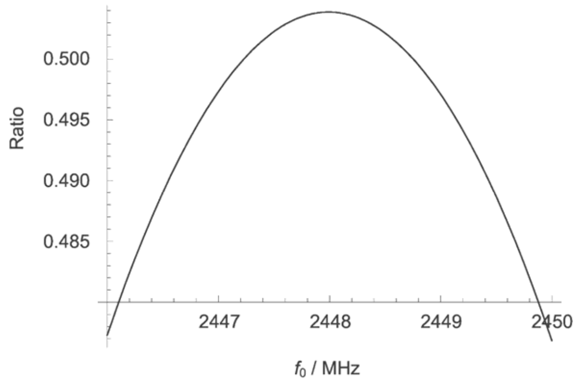

Fig. 5 Ratio between effective energy loss and total energy loss *vs*. f_0.

3.2 Omega3p simulation

Omega3p is a series of tools developed by Advanced Computational Department of SLAC and offers great accuracy. By using this software a design accurate to micron can be gotten. Q_0 is 3913.8 and Q_e is 298.1, so Q_L is 277.0. The electronics get about 52% of total energy loss in TM110 mode. Assume that *NF* of electronics is 10 and then the theoretical resolution can be gotten from equation (1)

$$\Delta x_{\text{theoretical}}=\left(\frac{NF}{0.52}\right)^{1/2}q^{-1}\left(\frac{\pi}{4kT}\frac{\beta}{1+\beta}k_{\text{loss, normalized}}\right)^{-1/2} \tag{14}$$

where $k_{\text{loss, normalized}} = 1.14\times10^{14}\ \Omega\cdot\text{m}^{-2}\cdot\text{s}^{-1}$

When bunch charge is 1 nC, the theoretical resolution is 7 nm and the final resolution is 31 nm. The external *Q* of monopole mode obtained from a simulation is 2.6×10^{13}, i.e. the monopole mode is successfully suppressed.

Since the whole system is symmetrical, all dipole modes can be expressed as a linear combination of two orthogonal dipole modes and coupled out by two pairs of waveguides (Fig. 6).

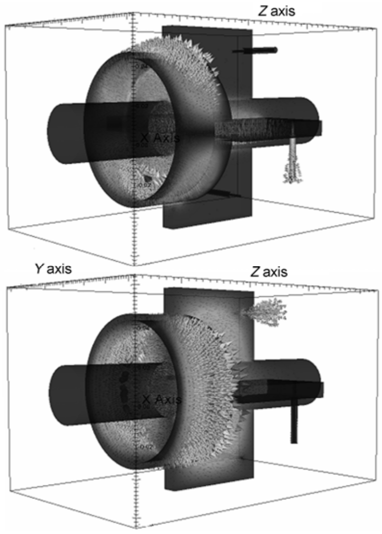

Fig. 6 Two orthogonal dipole modes, simulated by Omega3p.

Fig. 7 shows parameters of the design. The metal walls are not shown, because their thickness is changeable. Coaxial feed-through used in the design is SMA type feed through NL-108-546, produced by Hitachi Haramachi Electronics Co., Ltd.

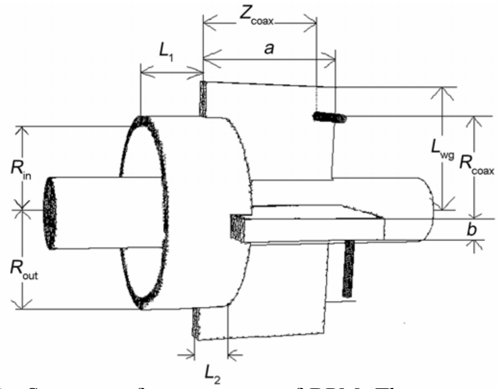

Fig. 7 Structure of vacuum part of BPM. The parameters (in mm) are: R_{in}, 44.000; R_{out}, 47.900; L_1, 30.304; L_2, 10.000; *a*, 70.000; *b*, 10.000; L_{wg}, 65.000; Z_{coax}, 55.060; and R_{coax}, 55.050.

4 Error analysis

Mechanical error can results in resonance frequency shifts and external *Q* changes. As showed in Fig. 5, the resonance frequency deviation from center frequency of electronics results in signal voltage decrease. A huge fall in external *Q* value of monopole mode results in larger leakage of monopole signal. So it is necessary to analyze it and give a machining tolerance.

4.1 Frequency and external Q variation of TM110 mode caused by mechanical error

From a simulation (Fig. 8), the resonance frequency of TM110 mode has a linear dependence on waveguide size (a, b and l_{wg} in Fig. 7) and length of coaxial extension to the cavity (L_1 in Fig. 7). Due to the result in Fig. 5, a general tolerance of 0.05 mm has been decided. Fig. 9 shows that the variation of external Q is about 1% of the design specification when waveguides are under given tolerance. The resulted signal voltage decrease is negligible. Actually, variation of external Q is always negligible unless the whole pick-up station is asymmetrical enough to cut off the dipole mode needed. So the frequency variation is more important.

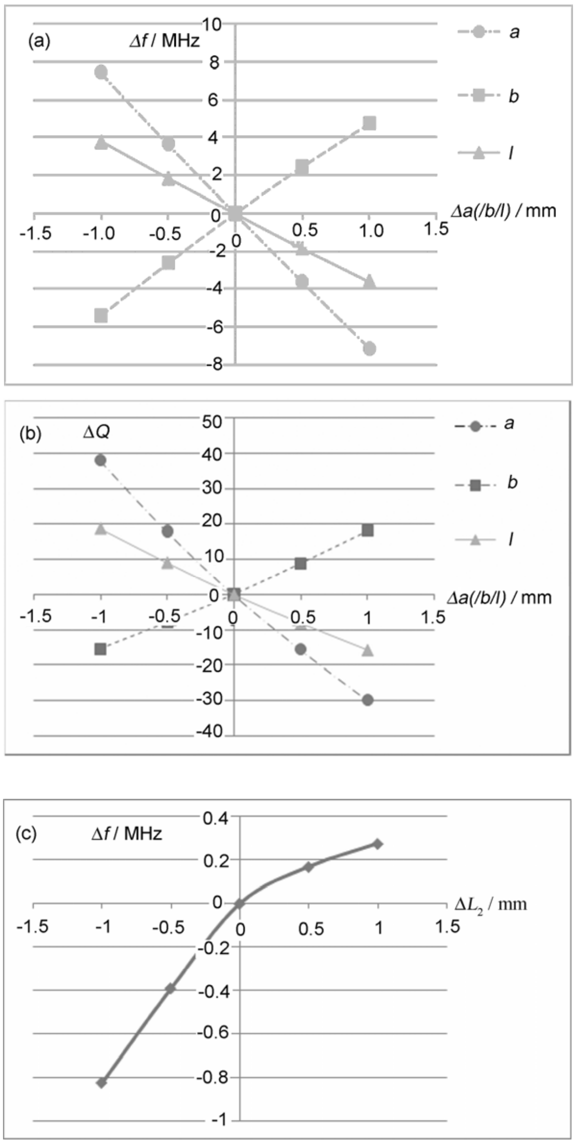

Fig. 8 Frequency variations of TM110 mode with the waveguide size (a), and the cavity shape (b) and thickness (c).

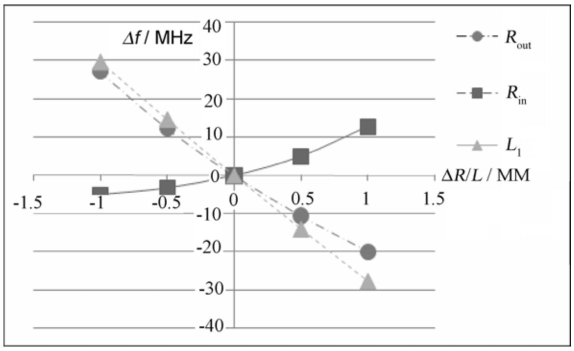

Fig. 9 External Q variations of TM110 mode with waveguide size.

As mentioned before, TM110 signal is proportionate to bunch displacement while the TM010 mode signal is invariable. Since the bunch displacement is very small, the TM010 signal is many orders of magnitude larger than the TM110 signal; therefore the measurement error is mainly caused by monopole leakage in addition to electronics noise.

In this design, two pairs of waveguides are used to couple two orthogonal dipole modes since the whole system is considered as symmetrical. If mechanical error induces asymmetry, there will be X-Y coupling, which means an X-orientation displacement may result in a Y-orientation reading.

Monopole leakage and X-Y coupling are mainly caused by mechanical misalignment and deformation. The deformation of whole system which could result in monopole leakage is unpredictable and cannot be quantitative analyzed, so only waveguide misalignment is analyzed here. Fig. 10 shows two kinds of waveguide installing misalignment.

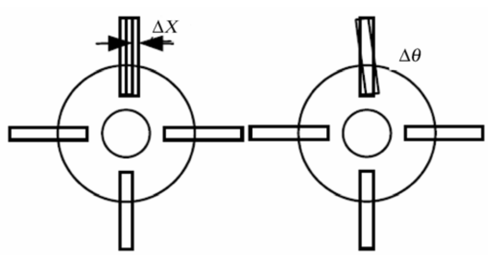

Fig. 10 Waveguide misalignment.

4.2 Monopole leakage caused by mechanical error

As showed in Fig. 2, the monopole leakage will not change when the waveguide rotates since the electromagnetic field of monopole mode is circular symmetrical. Therefore, only waveguide translation results in larger leakage.

Assuming a 1 mm waveguide translation, from a simulation by Omega3p, the external Q of monopole mode is 5.87×10^5, many orders of magnitude less than 2.6×10^{13}. By similar deduction as before,

$$\int_{-\infty}^{\infty} P(\omega)\mathrm{d}\omega = V_{010}^2 \frac{Q_L}{\pi\,\omega_{010}}\left(\frac{\pi}{2}-\left(-\frac{\pi}{2}\right)\right) = V_{010}^2\frac{Q_L}{\omega_{010}} = k_{\mathrm{loss}_{010}} q^2 \frac{\beta_{010}}{1+\beta_{010}} \tag{15}$$

$$E_{\mathrm{e}_{010}} = \int_{\omega_{110}-\pi\Delta F}^{\omega_{110}+\pi\Delta F} P(\omega)\mathrm{d}\omega = V_0^2\frac{Q_{L010}}{\pi\,\omega_{010}}\left[\mathrm{arctg}\left(\frac{\omega_{110}+2\pi\Delta F-\omega_{010}}{\omega_{010}/(2Q_{L010})}\right)-\mathrm{arctg}\left(\frac{\omega_{110}-2\pi\Delta F-\omega_{010}}{\omega_{010}/(2Q_{L010})}\right)\right] \tag{16}$$

The energy of TM010 mode detected by the electronics is then obtained. The offset caused by monopole mode is about 448 nm. This can be eliminated by off-line calibration.

4.3 *X-Y* coupling caused by mechanical error

Both rotation and translation can cause *X-Y* coupling. To calibrate the *X-Y* coupling, the external Q of one dipole mode in two different pairs of waveguides is compared. For example, without the *X-Y* coupling, the *X*-polarization dipole mode would couple to the *Y*-orientation waveguides, hence an external Q value of many orders of magnitude larger at X-orientation waveguides than the external Q at Y-orientation waveguides.

From simulations performed with three conditions: no translation or rotation, 1 mm waveguide translation and 1° rotation, the external Q of *X*-polarization at *Y*-orientation is around 300 under all the three conditions, while the external Q at *X*-orientation is always 10^5~10^6 under all conditions. So there is about 0.1% *X-Y* coupling, and the waveguide rotation and translation may affect the *X-Y* coupling, but not very seriously.

The *X-Y* coupling is linear coupling, first-order binary equations can be used for off-line calibration. A tolerance of 0.05 mm (§4.1) shall guarantee the whole system's good performance.

5 Electronics design

Though super heterodyne circuits are generally used in signal processing for cavity BPMs, chip AD8302 produced by Analog Devices is used to process the signals. Being able to give amplitude ratio and phase separation of two signals[9], AD8302 can be used to process the signals from position cavity and reference cavity and read the beam position exactly, with a thus simplified circuit—AD8302 processes signals in frequency of < 2.7 GHz and down-converter is not indispensable. The block diagram of electronics is shown in Fig. 11.

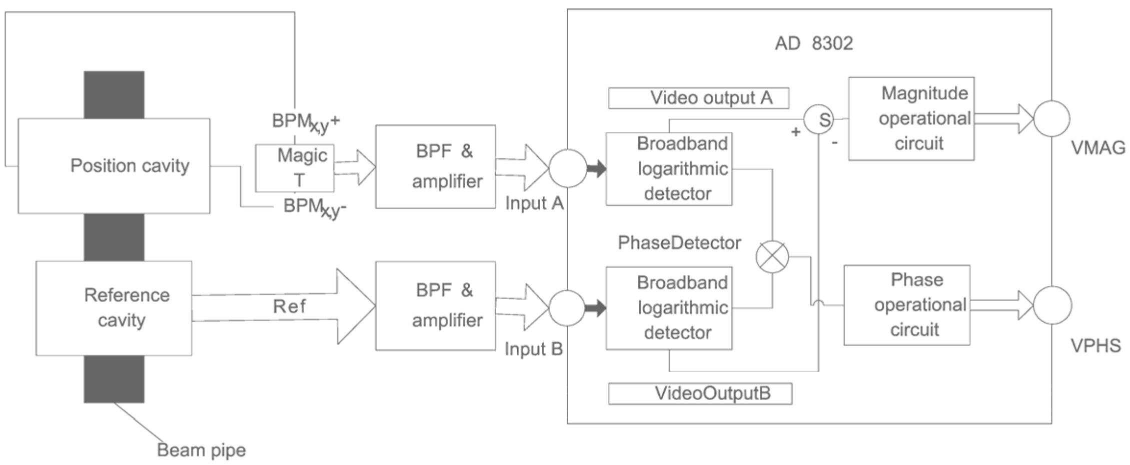

Fig. 11 Block diagram of electronics.

6 Conclusion

Since the ideal resolution of this design is 7 nm while the theoretical resolution is 31 nm when *NF*=10, it is possible to get an S-band cavity BPM system that has a high resolution less than 1μm. This is very useful for the new injector.

Acknowledgment

The authors would like to thank Dr. LI Zenghai and Advanced Computational Department of SLAC National Accelerator Laboratory for helps in this research.

References

1 LI Jihao, SUN Baogen, He Duohui, *et al*. HEP & NP (in Chinese), 2007, **31** (1): 96-100.

2 Sargsyan V. Tesla Reports, 2004, **3**: 1-9.

3 Slaton T, Mazaheri G, Shintake T. Development of nanometer resolution C-band radio frequency beam position monitors in the final focus test beam. Proc. of LINAC98. Chicago, 1998: 911-913.

4 Lorenz R. Cavity beam position monitors, Proc. of 1998 Beam Instrumentation Workshop. SLAC, Stanford, 1998: http://www.slac.stanford.edu/pubs/confproc/biw98/.

5 Maesaka H, Otake Y, Togowa K, *et al.* Beam position monitor at the SCSS prototype accelerator. Proc. of APAC 2007, Indore: 387-389.

6 Walston S, Boogert S, Chung Carl, *et al*. Nucl Inst Met Phy Res A, 2007, **578**: 1-22.

7 Lunin A, Romanov G, Solyak N, *et al*. Design of a submicron resolution cavity BPM for the ILC main linac. Proc. of the DIPAC’07, Venice, 2007: 192-194.

8 Li Z. S-band cavity BPM for ILC. The 2005 ILC Physics and Detector Workshop and 2nd ILC Accelerator Workshop (Snowmass 2005), 2005: http://www.hep.ucl.ac.uk/lc/T474/Documentation/ILCAW0901_TALK.PDF.

9 AD8302 Data Sheet: http://www.analog.com/static/imported-files/data_sheets/AD8302.pdf.